

World Journal of *Clinical Cases*

World J Clin Cases 2023 February 6; 11(4): 719-978



Contents

Thrice Monthly Volume 11 Number 4 February 6, 2023

MINIREVIEWS

- 719 Development and refinement of diagnostic and therapeutic strategies for managing patients with cardiogenic stroke: An arduous journey
Fan ZX, Liu RX, Liu GZ
- 725 Portal vein aneurysm-etiology, multimodal imaging and current management
Kurtcehajic A, Zerem E, Alibegovic E, Kunosic S, Hujdurovic A, Fejzic JA

ORIGINAL ARTICLE

Clinical and Translational Research

- 738 CD93 serves as a potential biomarker of gastric cancer and correlates with the tumor microenvironment
Li Z, Zhang XJ, Sun CY, Fei H, Li ZF, Zhao DB

Retrospective Study

- 756 Chest computed tomography findings of the Omicron variants of SARS-CoV-2 with different cycle threshold values
Ying WF, Chen Q, Jiang ZK, Hao DG, Zhang Y, Han Q
- 764 Major depressive disorders in patients with inflammatory bowel disease and rheumatoid arthritis
Haider MB, Basida B, Kaur J
- 780 Selective laser trabeculoplasty as adjunctive treatment for open-angle glaucoma *vs* following incisional glaucoma surgery in Chinese eyes
Zhu J, Guo J
- 788 Efficacy of transvaginal ultrasound-guided local injections of absolute ethanol for ectopic pregnancies with intrauterine implantation sites
Kakinuma T, Kakinuma K, Matsuda Y, Yanagida K, Ohwada M, Kaijima H

Clinical Trials Study

- 797 Efficacy of incremental loads of cow's milk as a treatment for lactose malabsorption in Japan
Hasegawa M, Okada K, Nagata S, Sugihara S

Observational Study

- 809 Transdiagnostic considerations of mental health for the post-COVID era: Lessons from the first surge of the pandemic
Goldstein Ferber S, Shoval G, Rossi R, Trezza V, Di Lorenzo G, Zalsman G, Weller A, Mann JJ
- 821 Effect of patient COVID-19 vaccine hesitancy on hospital care team perceptions
Caspi I, Freund O, Pines O, Elkana O, Ablin JN, Bornstein G

Randomized Clinical Trial

- 830** Improvement of inflammatory response and gastrointestinal function in perioperative of cholelithiasis by Modified Xiao-Cheng-Qi decoction
Sun BF, Zhang F, Chen QP, Wei Q, Zhu WT, Ji HB, Zhang XY

CASE REPORT

- 844** Metagenomic next-generation sequencing for pleural effusions induced by viral pleurisy: A case report
Liu XP, Mao CX, Wang GS, Zhang MZ
- 852** *Clostridium perfringens* gas gangrene caused by closed abdominal injury: A case report and review of the literature
Li HY, Wang ZX, Wang JC, Zhang XD
- 859** Is lymphatic invasion of microrectal neuroendocrine tumors an incidental event?: A case report
Ran JX, Xu LB, Chen WW, Yang HY, Weng Y, Peng YM
- 866** *Pneumocystis jirovecii* diagnosed by next-generation sequencing of bronchoscopic alveolar lavage fluid: A case report and review of literature
Cheng QW, Shen HL, Dong ZH, Zhang QQ, Wang YF, Yan J, Wang YS, Zhang NG
- 874** Identification of 1q21.1 microduplication in a family: A case report
Huang TT, Xu HF, Wang SY, Lin WX, Tung YH, Khan KU, Zhang HH, Guo H, Zheng G, Zhang G
- 883** Double pigtail catheter reduction for seriously displaced intravenous infusion port catheter: A case report
Liu Y, Du DM
- 888** Thyroid storm in a pregnant woman with COVID-19 infection: A case report and review of literatures
Kim HE, Yang J, Park JE, Baek JC, Jo HC
- 896** Computed tomography diagnosed left ovarian venous thrombophlebitis after vaginal delivery: A case report
Wang JJ, Hui CC, Ji YD, Xu W
- 903** Preoperative 3D reconstruction and fluorescent indocyanine green for laparoscopic duodenum preserving pancreatic head resection: A case report
Li XL, Gong LS
- 909** Unusual presentation of systemic lupus erythematosus as hemophagocytic lymphohistiocytosis in a female patient: A case report
Peng LY, Liu JB, Zuo HJ, Shen GF
- 918** Polyarteritis nodosa presenting as leg pain with resolution of positron emission tomography-images: A case report
Kang JH, Kim J
- 922** Easily misdiagnosed complex Klippel-Trenaunay syndrome: A case report
Li LL, Xie R, Li FQ, Huang C, Tuo BG, Wu HC

- 931 Benign lymphoepithelial cyst of parotid gland without human immunodeficiency virus infection: A case report
Liao Y, Li YJ, Hu XW, Wen R, Wang P
- 938 Epithelioid trophoblastic tumor of the lower uterine segment and cervical canal: A case report
Yuan LQ, Hao T, Pan GY, Guo H, Li DP, Liu NF
- 945 Treatment of portosystemic shunt-borne hepatic encephalopathy in a 97-year-old woman using balloon-occluded retrograde transvenous obliteration: A case report
Nishi A, Kenzaka T, Sogi M, Nakaminato S, Suzuki T
- 952 Development of Henoch-Schoenlein purpura in a child with idiopathic hypereosinophilia syndrome with multiple thrombotic onset: A case report
Xu YY, Huang XB, Wang YG, Zheng LY, Li M, Dai Y, Zhao S
- 962 Three cases of jejunal tumors detected by standard upper gastrointestinal endoscopy: A case series
Lee J, Kim S, Kim D, Lee S, Ryu K
- 972 Omental infarction diagnosed by computed tomography, missed with ultrasonography: A case report
Hwang JK, Cho YJ, Kang BS, Min KW, Cho YS, Kim YJ, Lee KS

ABOUT COVER

Editorial Board Member of *World Journal of Clinical Cases*, Sahand Samieirad, DDS, MS, MSc, Associate Professor, Oral and Maxillofacial Surgery Department, Mashhad Dental School, Mashhad University of Medical Sciences, Mashhad 9178613111, Iran. samieerads@mums.ac.ir

AIMS AND SCOPE

The primary aim of *World Journal of Clinical Cases* (WJCC, *World J Clin Cases*) is to provide scholars and readers from various fields of clinical medicine with a platform to publish high-quality clinical research articles and communicate their research findings online.

WJCC mainly publishes articles reporting research results and findings obtained in the field of clinical medicine and covering a wide range of topics, including case control studies, retrospective cohort studies, retrospective studies, clinical trials studies, observational studies, prospective studies, randomized controlled trials, randomized clinical trials, systematic reviews, meta-analysis, and case reports.

INDEXING/ABSTRACTING

The WJCC is now abstracted and indexed in Science Citation Index Expanded (SCIE, also known as SciSearch®), Journal Citation Reports/Science Edition, Current Contents®/Clinical Medicine, PubMed, PubMed Central, Scopus, Reference Citation Analysis, China National Knowledge Infrastructure, China Science and Technology Journal Database, and Superstar Journals Database. The 2022 Edition of Journal Citation Reports® cites the 2021 impact factor (IF) for WJCC as 1.534; IF without journal self cites: 1.491; 5-year IF: 1.599; Journal Citation Indicator: 0.28; Ranking: 135 among 172 journals in medicine, general and internal; and Quartile category: Q4. The WJCC's CiteScore for 2021 is 1.2 and Scopus CiteScore rank 2021: General Medicine is 443/826.

RESPONSIBLE EDITORS FOR THIS ISSUE

Production Editor: Si Zhao; Production Department Director: Xu Guo; Editorial Office Director: Jin-Lei Wang.

NAME OF JOURNAL

World Journal of Clinical Cases

ISSN

ISSN 2307-8960 (online)

LAUNCH DATE

April 16, 2013

FREQUENCY

Thrice Monthly

EDITORS-IN-CHIEF

Bao-Gan Peng, Jerzy Tadeusz Chudek, George Kontogeorgos, Maurizio Serati, Ja Hyeon Ku

EDITORIAL BOARD MEMBERS

<https://www.wjgnet.com/2307-8960/editorialboard.htm>

PUBLICATION DATE

February 6, 2023

COPYRIGHT

© 2023 Baishideng Publishing Group Inc

INSTRUCTIONS TO AUTHORS

<https://www.wjgnet.com/bpg/gerinfo/204>

GUIDELINES FOR ETHICS DOCUMENTS

<https://www.wjgnet.com/bpg/GerInfo/287>

GUIDELINES FOR NON-NATIVE SPEAKERS OF ENGLISH

<https://www.wjgnet.com/bpg/gerinfo/240>

PUBLICATION ETHICS

<https://www.wjgnet.com/bpg/GerInfo/288>

PUBLICATION MISCONDUCT

<https://www.wjgnet.com/bpg/gerinfo/208>

ARTICLE PROCESSING CHARGE

<https://www.wjgnet.com/bpg/gerinfo/242>

STEPS FOR SUBMITTING MANUSCRIPTS

<https://www.wjgnet.com/bpg/GerInfo/239>

ONLINE SUBMISSION

<https://www.f6publishing.com>



Retrospective Study

Chest computed tomography findings of the Omicron variants of SARS-CoV-2 with different cycle threshold values

Wei-Feng Ying, Qiong Chen, Zhi-Kui Jiang, Da-Guang Hao, Ying Zhang, Qian Han

Specialty type: Infectious diseases

Provenance and peer review:

Unsolicited article; Externally peer reviewed.

Peer-review model: Single blind

Peer-review report's scientific quality classification

Grade A (Excellent): 0
Grade B (Very good): B
Grade C (Good): 0
Grade D (Fair): 0
Grade E (Poor): 0

P-Reviewer: Shahid M, Pakistan

Received: September 1, 2022

Peer-review started: September 1, 2022

First decision: November 22, 2022

Revised: November 29, 2022

Accepted: January 12, 2023

Article in press: January 12, 2023

Published online: February 6, 2023



Wei-Feng Ying, Qiong Chen, Da-Guang Hao, Ying Zhang, Department of Radiology, Shanghai Xuhui Dahua Hospital, Shanghai 200237, China

Zhi-Kui Jiang, Qian Han, Department of Clinical Laboratory, Shanghai Xuhui Dahua Hospital, Shanghai 200237, China

Corresponding author: Qiong Chen, MSc, Chief Doctor, Department of Radiology, Shanghai Xuhui Dahua Hospital, No. 901 Lao'humun Road, Xuhui District, Shanghai 200237, China. cq1444@sina.com

Abstract

BACKGROUND

The Omicron variant of severe acute respiratory syndrome coronavirus 2 (SARS-CoV-2) mainly infects the upper respiratory tract. This study aimed to determine whether the probability of pulmonary infection and the cycle threshold (Ct) measured using the fluorescent polymerase chain reaction (PCR) method were related to pulmonary infections diagnosed *via* computed tomography (CT).

AIM

To analyze the chest CT signs of SARS-CoV-2 Omicron variant infections with different Ct values, as determined *via* PCR.

METHODS

The chest CT images and PCR Ct values of 331 patients with SARS-CoV-2 Omicron variant infections were retrospectively collected and categorized into low (< 25), medium (25.00-34.99), and high (≥ 35) Ct groups. The characteristics of chest CT images in each group were statistically analyzed.

RESULTS

The PCR Ct values ranged from 13.36 to 39.81, with 99 patients in the low, 155 in the medium, and 77 in the high Ct groups. Six abnormal chest CT signs were detected, namely, focal infection, patchy consolidation shadows, patchy ground-glass shadows, mixed consolidation ground-glass shadows, subpleural interstitial changes, and pleural changes. Focal infections were less frequent in the low Ct group than in the medium and high Ct groups; these infections were the most common sign in the medium and high Ct groups. Patchy consolidation shadows and pleural changes were more frequent in the low Ct group than in the other two groups. The number of patients with two or more signs was greater in the low Ct

group than in the medium and high Ct groups.

CONCLUSION

The chest CT signs of patients with pulmonary infection caused by the Omicron variants of SARS-CoV-2 varied depending on the Ct values. Identification of the characteristics of Omicron variant infection can help subsequent planning of clinical treatment.

Key Words: COVID-19; SARS-CoV-2; Omicron variant; Computed tomography; Cycle threshold; Polymerase chain reaction

©The Author(s) 2023. Published by Baishideng Publishing Group Inc. All rights reserved.

Core Tip: Pulmonary infections caused by the Omicron variant of severe acute respiratory syndrome coronavirus 2 were highly correlated with cycle threshold (Ct) values. Lower Ct values were associated with a higher incidence and degree of pulmonary damage.

Citation: Ying WF, Chen Q, Jiang ZK, Hao DG, Zhang Y, Han Q. Chest computed tomography findings of the Omicron variants of SARS-CoV-2 with different cycle threshold values. *World J Clin Cases* 2023; 11(4): 756-763

URL: <https://www.wjgnet.com/2307-8960/full/v11/i4/756.htm>

DOI: <https://dx.doi.org/10.12998/wjcc.v11.i4.756>

INTRODUCTION

Since the emergence of the Omicron variant of severe acute respiratory syndrome coronavirus 2 (SARS-CoV-2) on November 24, 2021[1], it has spread in most countries and caused infection in numerous individuals worldwide[2]. Although the virulence of Omicron appears to be weaker than that of previous SARS-CoV-2 variants, the large-scale use of vaccines against SARS-CoV-2, particularly with enhanced needles, has reduced the mortality rate associated with SARS-CoV-2[3]. Omicron is more infectious and transmissible than other variants[4,5] and causes damage to the lungs of some patients to different degrees[6]. Therefore, determining the degree of pulmonary damage caused by different Omicron viral load levels is key to understanding the characteristics of Omicron variant infection and its inhibition[7].

Fluorescent polymerase chain reaction (PCR) is the gold standard for diagnosing SARS-CoV-2 infection, and its cycle threshold (Ct) values can help achieve a reliable assessment and comparison of viral loads in patients[8-10]. Ct diagnosis has an extremely high diagnostic efficiency for determining the degree of pulmonary damage in patients with SARS-CoV-2 infections[11,12]. So far, only a few studies have attempted to correlate Ct values and pulmonary damage evidenced on chest computed tomography (CT) images obtained from patients with Omicron variant infection. The author's hospital is a designated treatment facility for symptomatic patients with Omicron variant infection. This study aimed to assess the chest CT signs of patients with Omicron variant infection with different Ct values for determining the severity of the infection and providing guidance for subsequent clinical treatments.

MATERIALS AND METHODS

Clinical data

Chest CT scans of patients with Omicron variant infection admitted to Shanghai Xuhui Dahua Hospital were collected from April to May 2022. The inclusion criteria were patients with PCR-positive results (Ct value of < 40) and those with viral infection signs on chest CT within 48 h after PCR. The exclusion criteria were patients with bacterial infections, as determined using laboratory indexes, or those with a clinical or CT diagnosis of other basic pulmonary infectious diseases. This study complied with the ethical standards and was approved by the Ethics Committee of Shanghai Xuhui Dahua Hospital (approval No. 20220804).

Examination method

All CT scans were obtained using a Siemens 64-slice spiral CT scanner (SOMATOM sensation) from the pulmonary apex to the pulmonary bottom using the following scanning parameters: Detector collimation, 64.0 mm × 0.6 mm; tube voltage, 120 KV; tube current, automatic milliamperere; slice thickness, 5 mm; reconstructed slice thickness, 1.5 mm; reconstructed slice spacing, 1.5 mm; and matrix,

512 × 512.

Image analysis

The lower Ct value between the ORF and N genes was selected as the PCR Ct value. The patients were divided into three groups based on their Ct values: Low (< 25), medium (25.00-34.99), and high (≥ 35) Ct groups. Double-blind analysis was conducted using the CT data of each group by two physicians with > 10 years of experience in radiological diagnosis. In cases of disagreement, consensus was achieved after mutual consultation. When patients exhibited pulmonary infection foci with a long diameter (≤ 20 mm), it was considered as a focal infection. Other infection signs, including patchy consolidation shadows, patchy ground-glass density shadows, subpleural interstitial changes, mixed consolidation ground-glass shadows, and pleural changes, were judged based on their characteristics.

Statistical methods

Statistical analysis of the data was performed using SPSS 23.0. Normally distributed data are expressed as mean ± SD, whereas enumeration data are expressed as case numbers or percentages. Within- and between-group comparisons of CT signs were performed using χ^2 test. A *P* value of < 0.05 was considered to indicate statistical significance.

RESULTS

Baseline characteristics

Chest CT images of 331 patients [143 men and 188 women; age: 76 ± 12 (range: 25-102) years] with Omicron variant infection were collected. All patients showed respiratory symptoms of varying degrees, mainly including fever ($n = 247$, 74.62%), cough ($n = 203$, 61.33%), and chest tightness ($n = 49$, 14.8%). Among them, 187 (56.5%) patients were vaccinated thrice against SARS-CoV-2, 74 (22.36%) were vaccinated twice, 12 (3.63%) were vaccinated once, and 58 (17.52%) were not vaccinated. Additionally, 236 (71.3%) patients had a history of close or secondary contact with patients with SARS-CoV-2 infection, 65 (19.64%) had a definite history of gathering in public places, and 30 (9.06%) had no definite history of close contact with patients with SARS-CoV-2 infection.

The PCR Ct values ranged from 13.36 to 39.81 (average, 28.85 ± 6.68), with 99 (29.91%) patients in the low, 155 (46.83%) in the medium, and 77 (23.26%) in the high Ct groups.

General distribution of abnormal chest CT characteristics

Among all patients, the most common CT sign was focal infection ($n = 178$, 45.18%), followed by subpleural interstitial changes ($n = 81$, 20.56%), patchy ground-glass density shadows ($n = 76$, 19.29%), patchy consolidation shadows ($n = 27$, 6.85%), pleural changes ($n = 20$, 5.08%), and mixed consolidation ground-glass shadows ($n = 12$, 3.04%).

Analysis of the differences in the distribution of abnormal chest CT characteristics within and between different Ct groups

Focal infections were less frequent in the low Ct group (30%) than in the medium (52.27%, $\chi^2 = 10.004$, $P = 0.002$) and high (53.41%, $\chi^2 = 10.895$, $P = 0.002$) Ct groups. Focal infection was the most common sign in the medium and high Ct groups (compared with the second most common sign in the groups: The medium Ct group, $\chi^2 = 23.780$, $P < 0.001$ and the high Ct group, $\chi^2 = 19.100$, $P < 0.001$), with statistically significant differences (Figure 1A-C).

The frequency of patchy consolidation shadows (Figure 1D-F) was the highest in the low Ct group (14.62%), less in the medium Ct group (3.98%; $\chi^2 = 7.037$, $P = 0.014$), and the lowest in the high Ct group (1.14%), with statistically significant between-group differences ($\chi^2 = 13.315$, $P < 0.001$).

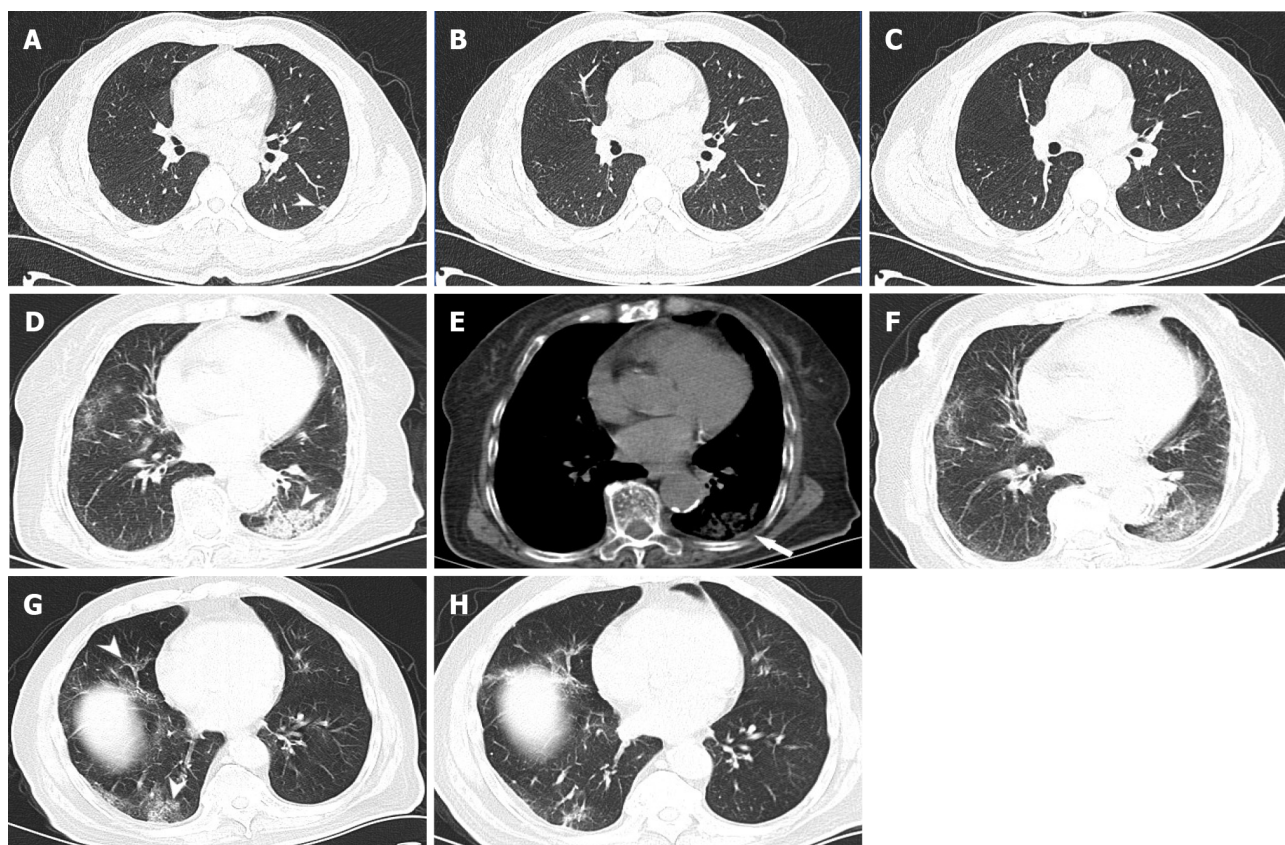
There were no statistically significant differences in the frequency of patchy ground-glass density shadows (Figure 1G and H) among the low (16.92%), medium (19.32%), and high (22.73%) Ct groups ($\chi^2 = 0.136$, $\chi^2 = 1.125$, and $\chi^2 = 0.482$; $P = 0.854$, $P = 0.377$, and $P = 0.603$, respectively).

Furthermore, no statistically significant differences were observed in subpleural interstitial changes among the low (25.38%), medium (17.61%), and high (19.32%) Ct groups ($\chi^2 = 1.452$, $\chi^2 = 1.049$, and $\chi^2 = 0.033$; $P = 0.302$, $P = 0.394$, and $P = 1.000$, respectively).

In addition, mixed consolidation ground-glass shadows showed no statistically significant differences among the low (2.31%), medium (3.98%), and high (2.27%) Ct groups ($\chi^2 = 0.687$, $\chi^2 = 0.000$, and $\chi^2 = 0.687$; $P = 0.683$, $P = 1.000$, and $P = 0.683$, respectively).

The frequency of pleural changes (Figure 1D-F) was the highest in the low Ct group (10.77%), less frequent in the medium Ct group (2.84%; $\chi^2 = 4.916$, $P = 0.049$), and the lowest in the high Ct group (1.13%; $\chi^2 = 8.865$, $P < 0.005$), with statistically significant between-group differences.

Among the three groups, the number of patients with two or more abnormal chest CT signs was the highest in the low Ct group (30.3%, 30/99), less in the medium Ct group [12.26% (19/155), $\chi^2 = 9.765$, $P = 0.003$], and the lowest in the high Ct group [12.99% (10/77), $\chi^2 = 8.562$, $P = 0.005$], with statistically



DOI: 10.12998/wjcc.v11.i4.756 Copyright ©The Author(s) 2023.

Figure 1 Computed tomography. A and B: A 48-year-old man had a history of close contact with patients mildly infected with SARS-CoV-2 Omicron variant. He had fever and mild cough for 3 d, with nucleic acid polymerase chain reaction positivity [cycle threshold (Ct) value, 35.43], leukocyte count of $7.26 \times 10^9/L$, neutrophil proportion of 58.8%, lymphocyte proportion of 32.9%, hypersensitive C-reactive protein content of $< 0.5 \text{ mg/L}$ (reference range, 0–8), and serum amyloid A (rapid method) content of $< 5.0 \text{ mg/L}$ (reference value < 10). The pulmonary window of the chest computed tomography (CT) scan revealed a focal high-density infection in the long diameter of the dorsal segment of the left lower lobe ($< 2 \text{ cm}$) (A, short arrow); CT re-examination after 4 d revealed a decreased lesion density and slightly increased volume in the dorsal segment of the left lower lobe (B); 1 wk later, CT images showed that most of the lesions were dissipated and absorbed (C); D–F: A 93-year-old woman had a history of close contact with asymptomatic patients infected with SARS-CoV-2 Omicron variant. She had a high fever, cough, and expectoration for 4 d, with nucleic acid polymerase chain reaction positivity (Ct value, 23.97), leukocyte count of $7.41 \times 10^9/L$, neutrophil proportion of 63.3%, lymphocyte proportion of 22.25% (close to the lower limit of normal value), hypersensitive C-reactive protein content of 31.48 mg/L ↑, serum amyloid A (rapid method) content of $> 200 \text{ mg/L}$ ↑, partial pressure of carbon dioxide of $4.65 \downarrow$, and D-dimer content of $4.25 \uparrow$. The pulmonary window of the chest CT scan revealed consolidation shadows in the dorsal segment of the left lower lobe (short arrow) accompanied with a small amount of effusion in the adjacent pleural cavity, and scattered patchy, slightly high-density infection foci in both lungs, suggestive of an infection (D); the mediastinal window of the same CT revealed a small amount of effusion in the left pleural cavity (long arrow) (E); CT re-examination after 5 d revealed a decreased density of the consolidation infection foci in the dorsal segment of the left lower lobe and partial absorption of other infection foci in both lungs (F); G and H: An 81-year-old man had a history of close contact with his wife who had asymptomatic SARS-CoV-2 Omicron infection. He had fever, cough, and expectoration for 4 d, with nucleic acid polymerase chain reaction positivity (Ct value, 26.3), leukocyte count of $7.73 \times 10^9/L$, neutrophil proportion of 61.9%, lymphocyte proportion of 20.1% (close to the lower limit of normal value), hypersensitive C-reactive protein content of 7.42 mg/L , and serum amyloid A (rapid method) content of 16.6 mg/L ↑. The pulmonary window of the chest CT scan revealed scattered patchy ground-glass density shadows in the right middle and lower lobes (short arrows) (G); CT re-examination after 6 d revealed shrinkage and partial absorption of most of the infected foci in the right lung (H).

significant between-group differences (Table 1).

DISCUSSION

SARS-CoV-2 is constantly mutating. A recent report in *Lancet* confirmed that the viral genomes of the current round of local viral epidemics in Shanghai (present since late February) consist of the SARS-CoV-2 BA.2.2 variant, which is a subpopulation of the SARS-CoV-2 Omicron variant (B.1.1.159)[13]. Although its virulence is weaker than that of previous variants (including the Delta variant), it exhibits higher infectivity and stronger ability to escape the immune system, resulting in large-scale infections, high Ct values among symptomatic patients, and high mortality rates, which have an impact on the society. Therefore, it is particularly important to understand the clinical manifestations and imaging characteristics of patients with Omicron variant infection.

Table 1 Differences in the distribution of abnormal chest computed tomography imaging characteristics in each cycle threshold group, *n* = 394

Group	CT sign						Total
	Focal infection	Patchy consolidation shadows	Patchy ground-glass density shadows	Mixed consolidation ground-glass shadows	Subpleural interstitial changes	Pleural changes	
Low Ct group (< 25)	39 ¹	19 ²	22	3	33	14 ²	130
Medium Ct group (25.00-34.99)	92 ¹	7	34	7	31	5	176
High Ct group (≥ 35)	47 ¹	1	20	2	17	1	88
Total	178	27	76	12	81	20	394

¹Statistically significant difference in the group;²Statistically significant difference between groups.

CT: Computed tomography; Ct: Cycle threshold.

Currently, the autopsy reports of patients with Omicron variant infection are rarely reported; therefore, the pathological mechanism of this infection remains unclear. According to the autopsy reports of other SARS-CoV-2 subtypes abroad[14-16], SARS-CoV-2 directly infects target cells, including bronchial and alveolar epithelial cells, vascular epithelial and endothelial cells, and immune cells. The formation of early vasculitis leads to vascular wall and perivascular inflammation, immune cell infiltration, vascular stenosis, thrombosis, and secondary bleeding. In the later stage of SARS-CoV-2 infection, interstitial fibrosis and diffuse alveolar injury of the perivascular lung parenchyma can often occur secondary to infection with various bacteria and mucor, consolidation, and complications, such as mucus plugs formed by airway mucus secretion and peripheral pleural changes. Viruses can travel through the blood and induce pathological changes in other parts of the body.

PCR Ct values indicate the number of amplifications required for detecting SARS-CoV-2. The lower the Ct value, the higher the viral load in a nucleic acid sample and vice versa. A previous study reported a linear correlation between Ct values and viral loads. Accordingly, Ct values can reflect the viral levels in patients to a certain extent[8,10]. Some studies have considered Ct values of < 25 to indicate high viral loads; these patients required a longer viral clearance time[17]. We included patients with Ct values of < 25 in the low Ct group. According to the Diagnosis and Treatment Protocol for Novel Coronavirus Pneumonia (Trial Version 9) of China, the standard for dissolution in our region was a Ct value of ≥ 35. Moreover, another study reported that the virus can no longer be isolated from samples at Ct values ≥ 35[18]. Thus, we included patients with Ct values ≥ 35 and < 25 in the high and low Ct groups, respectively. Patients with Ct values of 25.00-34.99 were included in the medium Ct group. Along with chest CT features, Ct values can help improve our understanding of the pathological characteristics of patients with Omicron variant infection.

In this study, among all groups, the most common abnormal chest CT sign was focal infection (30.00%-53.41%, all *P* < 0.05), which was observed as blurred shadows, consolidation shadows, ground-glass density shadows with a long diameter (≤ 2 cm), and small nodule-like shadows with fuzzy edges, most of which were located under the pleura. These findings differ from the most common abnormal sign (patchy ground-glass density shadows) observed in patients with other previously identified SARS-CoV-2 subtype infection[19]. This suggests that the virulence of the Omicron variant is weaker than that of other SARS-CoV-2 variants. In addition, the large-scale use of vaccines leads to the most infection-caused vasculitis being replaced by peripheral vasculitis, more limited secondary peripheral pathological changes, and more common focal infections in the medium and high Ct groups. These findings indicate that lower viral loads in patients with Omicron variant infection result in fewer pulmonary infection foci and improved prognosis.

Among all Ct groups, patchy ground-glass density shadows (16.92%-22.73%) and subpleural interstitial changes (17.61%-25.38%) were also common (but not the most common) chest CT signs. Mixed consolidation ground-glass shadows were less common (2.27%-3.98%). In addition, the above abnormal signs were not significantly different among the three groups (all *P* > 0.05). These abnormal signs were consistent with the chest CT findings of pneumonia caused by other SARS-CoV-2 variants [20-22], however, their proportions were significantly decreased, indicating that the virulence of Omicron is weaker than that of previously identified variants.

The number of patients with patchy consolidation shadows (14.62%), pleural changes (10.77%), and two or more abnormal signs (30.3%) was higher in the low Ct group than in the other two groups (all *P*

< 0.05). Overall, Omicron infection showed fewer signs of pulmonary consolidation than other SARS-CoV-2 variant infections[23]. Consolidation shadows may result from vasculitis, hemorrhage, and peripheral serous exudation caused by high viral loads attacking blood vessels, secondary or direct alveolar inflammation, massive immune cell filling, and small airway mucus plugs. In addition, exudative and inflammatory stimulation of some lesions induces changes such as pleural thickening and pleural effusion. These results suggest that high viral loads can lead to severe and complex pulmonary injuries in some patients.

We used a Ct value of ≥ 35 as an inclusion criterion for patients in the high Ct group. Ct values of ≥ 35 in two consecutive tests is a criterion for patient discharge from mobile cabin hospitals, according to the Diagnosis and Treatment Plan for SARS-CoV-2 Pneumonia (trial version 9) issued by the National Health Commission of the People's Republic of China. Although such patients are noninfectious, their lungs might show abnormal signs to different degrees. Therefore, follow-up observations and treatment of such patients is important.

The sample size of this study was reasonable. Although future studies should be conducted with larger sample sizes, considering the urgent epidemic situation, the sample size of this study was adequate. It is expected that studies with a large sample size will further validate our findings.

CONCLUSION

In this study, patients with SARS-CoV-2 Omicron variant infection were grouped based on their Ct values. We found that the chest CT signs of patients with different viral loads varied to a certain extent. Focal infection was the most common abnormal chest CT sign in the medium and high Ct groups. Patients in the high Ct group more commonly presented with patchy consolidation shadows, pleural changes, and two or more abnormal CT signs than those in the other two groups. The results of this study can effectively enhance our understanding of the characteristics of Omicron variant infections and provide guidance for subsequent clinical treatments of patients with such infections.

ARTICLE HIGHLIGHTS

Research background

The Omicron variant of severe acute respiratory syndrome coronavirus 2 (SARS-CoV-2) mainly infects the upper respiratory tract. Chest computed tomography (CT) can reveal the presence of pulmonary infection. The measured cycle threshold (Ct) was related to pulmonary infections diagnosed *via* CT.

Research motivation

To explore the relationship between chest CT characteristics and Ct value using the fluorescent polymerase chain reaction (PCR) method.

Research objectives

Pulmonary infections caused by the Omicron variant of severe acute respiratory syndrome coronavirus 2 were highly correlated with Ct values. Lower Ct values were associated with a higher incidence and degree of pulmonary damage.

Research methods

The chest CT images and PCR Ct values of 331 patients with Omicron variant infections were retrospectively collected; categorized into low (< 25), moderate (25.00-34.99), and high (≥ 35) Ct groups; and analyzed statistically.

Research results

Focal infections were less frequent in the low Ct group than in the medium and high Ct groups. Patchy consolidation shadows and pleural changes were more common in the low Ct group than in the other two groups. The number of patients with two or more signs was greater in the low Ct group than in the medium and high Ct groups.

Research conclusions

Pulmonary infection and the Ct measured using the fluorescent PCR method were related to pulmonary infections diagnosed *via* CT.

Research perspectives

Future studies with large sample sizes and multiple centers will further validate our findings.

FOOTNOTES

Author contributions: Chen Q designed the research study; Jiang ZK and Han Q performed the research; Hao DG and Zhang Y contributed new reagents and analytic tools; Ying WF analyzed the data and wrote the manuscript; All authors have read and approved the final manuscript.

Institutional review board statement: This study was reviewed and approved by the Ethics Committee of Shanghai Xuhui Dahua Hospital (Approval No. 20220804).

Informed consent statement: All study participants or their legal guardian provided informed written consent about personal and medical data collection prior to study enrolment.

Conflict-of-interest statement: The authors state that there are no conflicts of interest to report.

Data sharing statement: Technical appendix, statistical code, and dataset available from the corresponding author at cq1444@sina.com upon reasonable request.

Open-Access: This article is an open-access article that was selected by an in-house editor and fully peer-reviewed by external reviewers. It is distributed in accordance with the Creative Commons Attribution NonCommercial (CC BY-NC 4.0) license, which permits others to distribute, remix, adapt, build upon this work non-commercially, and license their derivative works on different terms, provided the original work is properly cited and the use is non-commercial. See: <https://creativecommons.org/licenses/by-nc/4.0/>

Country/Territory of origin: China

ORCID number: Wei-Feng Ying 0000-0002-8877-6828; Qiong Chen 0000-0001-7167-1897; Zhi-Kui Jiang 0000-0003-2716-2790; Da-Guang Hao 0000-0002-1386-8189; Ying Zhang 0000 0002 1386 8189; Qian Han 0000-0002-1138-3284.

Corresponding Author's Membership in Professional Societies: Member of tumor imaging special committee of Shanghai anticancer association Member of Shanghai radiologist Association.

S-Editor: Chen YL

L-Editor: Filipodia

P-Editor: Chen YL

REFERENCES

- 1 Meo SA, Meo AS, Al-Jassir FF, Klonoff DC. Omicron SARS-CoV-2 new variant: global prevalence and biological and clinical characteristics. *Eur Rev Med Pharmacol Sci* 2021; **25**: 8012-8018 [PMID: 34982465 DOI: 10.26355/eurrev_202112_27652]
- 2 Nyberg T, Ferguson NM, Nash SG, Webster HH, Flaxman S, Andrews N, Hinsley W, Bernal JL, Kall M, Bhatt S, Blomquist P, Zaidi A, Volz E, Aziz NA, Harman K, Funk S, Abbott S; COVID-19 Genomics UK (COG-UK) consortium, Hope R, Charlett A, Chand M, Ghani AC, Seaman SR, Dabrera G, De Angelis D, Presanis AM, Thelwall S. Comparative analysis of the risks of hospitalisation and death associated with SARS-CoV-2 omicron (B.1.1.529) and delta (B.1.617.2) variants in England: a cohort study. *Lancet* 2022; **399**: 1303-1312 [PMID: 35305296 DOI: 10.1016/S0140-6736(22)00462-7]
- 3 Pérez-Then E, Lucas C, Monteiro VS, Miric M, Brache V, Cochon L, Vogels CBF, Malik AA, De la Cruz E, Jorge A, De Los Santos M, Leon P, Breban MI, Billig K, Yildirim I, Pearson C, Downing R, Gagnon E, Muyombwe A, Razeq J, Campbell M, Ko AI, Omer SB, Grubaugh ND, Vermund SH, Iwasaki A. Neutralizing antibodies against the SARS-CoV-2 Delta and Omicron variants following heterologous CoronaVac plus BNT162b2 booster vaccination. *Nat Med* 2022; **28**: 481-485 [PMID: 35051990 DOI: 10.1038/s41591-022-01705-6]
- 4 Garcia-Beltran WF, St Denis KJ, Hoelzemer A, Lam EC, Nitido AD, Sheehan ML, Berrios C, Ofoman O, Chang CC, Hauser BM, Feldman J, Roederer AL, Gregory DJ, Poznansky MC, Schmidt AG, Iafrate AJ, Naranbhai V, Balazs AB. mRNA-based COVID-19 vaccine boosters induce neutralizing immunity against SARS-CoV-2 Omicron variant. *Cell* 2022; **185**: 457-466.e4 [PMID: 34995482 DOI: 10.1016/j.cell.2021.12.033]
- 5 Chen J, Wang R, Gilby NB, Wei GW. Omicron Variant (B.1.1.529): Infectivity, Vaccine Breakthrough, and Antibody Resistance. *J Chem Inf Model* 2022; **62**: 412-422 [PMID: 34989238 DOI: 10.1021/acs.jcim.1c01451]
- 6 Kozlov M. Omicron's feeble attack on the lungs could make it less dangerous. *Nature* 2022; **601**: 177 [PMID: 34987210 DOI: 10.1038/d41586-022-00007-8]
- 7 Ren SY, Wang WB, Gao RD, Zhou AM. Omicron variant (B.1.1.529) of SARS-CoV-2: Mutation, infectivity, transmission, and vaccine resistance. *World J Clin Cases* 2022; **10**: 1-11 [PMID: 35071500 DOI: 10.12998/wjcc.v10.i1.1]
- 8 Garrett N, Tapley A, Andriessen J, Seocharan I, Fisher LH, Bunts L, Espy N, Wallis CL, Randhawa AK, Ketter N, Yacovone M, Goga A, Bekker LG, Gray GE, Corey L. High Rate of Asymptomatic Carriage Associated with Variant Strain Omicron. *medRxiv* 2022 [PMID: 35043118 DOI: 10.1101/2021.12.20.21268130]
- 9 Osterman A, Badell I, Basara E, Stern M, Kriesel F, Eleteby M, Öztan GN, Huber M, Autenrieth H, Knabe R, Späth PM, Muenchhoff M, Graf A, Krebs S, Blum H, Durner J, Czibere L, Dächert C, Kaderali L, Baldauf HM, Keppler OT. Impaired detection of omicron by SARS-CoV-2 rapid antigen tests. *Med Microbiol Immunol* 2022; **211**: 105-117 [PMID: 35187580]

- DOI: [10.1007/s00430-022-00730-z](https://doi.org/10.1007/s00430-022-00730-z)]
- 10 **Juanola-Falgarona M**, Peñarrubia L, Jiménez-Guzmán S, Porco R, Congost-Teixidor C, Varo-Velázquez M, Rao SN, Pueyo G, Manissero D, Pareja J. Ct values as a diagnostic tool for monitoring SARS-CoV-2 viral load using the QIAstat-Dx® Respiratory SARS-CoV-2 Panel. *Int J Infect Dis* 2022; **122**: 930-935 [PMID: [35840097](https://pubmed.ncbi.nlm.nih.gov/35840097/) DOI: [10.1016/j.ijid.2022.07.022](https://doi.org/10.1016/j.ijid.2022.07.022)]
 - 11 **Tsakok MT**, Watson RA, Saujani SJ, Kong M, Xie C, Peschl H, Wing L, MacLeod FK, Shine B, Talbot NP, Benamore RE, Eyre DW, Gleeson F. Reduction in Chest CT Severity and Improved Hospital Outcomes in SARS-CoV-2 Omicron Compared with Delta Variant Infection. *Radiology* 2023; **306**: 261-269 [PMID: [35727150](https://pubmed.ncbi.nlm.nih.gov/35727150/) DOI: [10.1148/radiol.220533](https://doi.org/10.1148/radiol.220533)]
 - 12 **Yoon SH**, Lee JH, Kim BN. Chest CT Findings in Hospitalized Patients with SARS-CoV-2: Delta versus Omicron Variants. *Radiology* 2023; **306**: 252-260 [PMID: [35762887](https://pubmed.ncbi.nlm.nih.gov/35762887/) DOI: [10.1148/radiol.220676](https://doi.org/10.1148/radiol.220676)]
 - 13 **Zhang X**, Zhang W, Chen S. Shanghai's life-saving efforts against the current omicron wave of the COVID-19 pandemic. *Lancet* 2022; **399**: 2011-2012 [PMID: [35533708](https://pubmed.ncbi.nlm.nih.gov/35533708/) DOI: [10.1016/S0140-6736\(22\)00838-8](https://doi.org/10.1016/S0140-6736(22)00838-8)]
 - 14 **Goussard P**, Schubert P, Parker N, Myburgh C, Rabie H, van der Zalm MM, Van Zyl GU, Preiser W, Maponga TG, Verster J, Gie AG, Andronikou S. Fatal SARS-CoV-2 Omicron variant in a young infant: Autopsy findings. *Pediatr Pulmonol* 2022; **57**: 1363-1365 [PMID: [35243813](https://pubmed.ncbi.nlm.nih.gov/35243813/) DOI: [10.1002/ppul.25881](https://doi.org/10.1002/ppul.25881)]
 - 15 **Martín-Martín J**, Martín-Cazorla F, Suárez J, Rubio L, Martín-de-Las-Heras S. Comorbidities and autopsy findings of COVID-19 deaths and their association with time to death: a systematic review and meta-analysis. *Curr Med Res Opin* 2022; **38**: 785-792 [PMID: [35254193](https://pubmed.ncbi.nlm.nih.gov/35254193/) DOI: [10.1080/030077995.2022.2050110](https://doi.org/10.1080/030077995.2022.2050110)]
 - 16 **Calabrese F**, Pezzuto F, Fortarezza F, Hofman P, Kern I, Panizo A, von der Thüsen J, Timofeev S, Gorkiewicz G, Lunardi F. Pulmonary pathology and COVID-19: lessons from autopsy. The experience of European Pulmonary Pathologists. *Virchows Arch* 2020; **477**: 359-372 [PMID: [32642842](https://pubmed.ncbi.nlm.nih.gov/32642842/) DOI: [10.1007/s00428-020-02886-6](https://doi.org/10.1007/s00428-020-02886-6)]
 - 17 **Aranha C**, Patel V, Bhor V, Gogoi D. Cycle threshold values in RT-PCR to determine dynamics of SARS-CoV-2 viral load: An approach to reduce the isolation period for COVID-19 patients. *J Med Virol* 2021; **93**: 6794-6797 [PMID: [34264527](https://pubmed.ncbi.nlm.nih.gov/34264527/) DOI: [10.1002/jmv.27206](https://doi.org/10.1002/jmv.27206)]
 - 18 **Ke R**, Martinez PP, Smith RL, Gibson LL, Mirza A, Conte M, Gallagher N, Luo CH, Jarrett J, Zhou R, Conte A, Liu T, Farjo M, Walden KKO, Rendon G, Fields CJ, Wang L, Fredrickson R, Edmonson DC, Baughman ME, Chiu KK, Choi H, Scardina KR, Bradley S, Gloss SL, Reinhart C, Yedetore J, Quicksall J, Owens AN, Broach J, Barton B, Lazar P, Heetderks WJ, Robinson ML, Mostafa HH, Manabe YC, Pekosz A, McManus DD, Brooke CB. Daily longitudinal sampling of SARS-CoV-2 infection reveals substantial heterogeneity in infectiousness. *Nat Microbiol* 2022; **7**: 640-652 [PMID: [35484231](https://pubmed.ncbi.nlm.nih.gov/35484231/) DOI: [10.1038/s41564-022-01105-z](https://doi.org/10.1038/s41564-022-01105-z)]
 - 19 **Solomon JJ**, Heyman B, Ko JP, Condos R, Lynch DA. CT of Post-Acute Lung Complications of COVID-19. *Radiology* 2021; **301**: E383-E395 [PMID: [34374591](https://pubmed.ncbi.nlm.nih.gov/34374591/) DOI: [10.1148/radiol.2021211396](https://doi.org/10.1148/radiol.2021211396)]
 - 20 **Chinese Research Hospital Association**; Respiratory Council. [Expert recommendations for the diagnosis and treatment of interstitial lung disease caused by novel coronavirus pneumonia]. *Zhonghua Jie He He Hu Xi Za Zhi* 2020; **43**: 827-833 [PMID: [32992435](https://pubmed.ncbi.nlm.nih.gov/32992435/) DOI: [10.3760/cma.j.cn112147-20200326-00419](https://doi.org/10.3760/cma.j.cn112147-20200326-00419)]
 - 21 **Hu Q**, Guan H, Sun Z, Huang L, Chen C, Ai T, Pan Y, Xia L. Early CT features and temporal lung changes in COVID-19 pneumonia in Wuhan, China. *Eur J Radiol* 2020; **128**: 109017 [PMID: [32387924](https://pubmed.ncbi.nlm.nih.gov/32387924/) DOI: [10.1016/j.ejrad.2020.109017](https://doi.org/10.1016/j.ejrad.2020.109017)]
 - 22 **Yan S**, Chen H, Xie RM, Guan CS, Xue M, Lv ZB, Wei LG, Bai Y, Chen BD. Chest CT Evaluation of 11 Persistent Asymptomatic Patients with SARS-CoV-2 Infection. *Jpn J Infect Dis* 2021; **74**: 1-6 [PMID: [32611980](https://pubmed.ncbi.nlm.nih.gov/32611980/) DOI: [10.7883/yoken.JJID.2020.264](https://doi.org/10.7883/yoken.JJID.2020.264)]
 - 23 **Granata V**, Fusco R, Villanacci A, Magliocchetti S, Urraro F, Tetaj N, Marchioni L, Albarello F, Campioni P, Cristofaro M, Di Stefano F, Fusco N, Petrone A, Schinà V, Grassi F, Girardi E, Ianniello S. Imaging Severity COVID-19 Assessment in Vaccinated and Unvaccinated Patients: Comparison of the Different Variants in a High Volume Italian Reference Center. *J Pers Med* 2022; **12** [PMID: [35743740](https://pubmed.ncbi.nlm.nih.gov/35743740/) DOI: [10.3390/jpm12060955](https://doi.org/10.3390/jpm12060955)]



Published by **Baishideng Publishing Group Inc**
7041 Koll Center Parkway, Suite 160, Pleasanton, CA 94566, USA

Telephone: +1-925-3991568

E-mail: bpgoffice@wjgnet.com

Help Desk: <https://www.f6publishing.com/helpdesk>

<https://www.wjgnet.com>

